Materials Today: Proceedings 38 (2021) 1191–1196

Contents lists available at ScienceDirect

Materials Today: Proceedings

journal homepage: www.elsevier.com/locate/matpr

Nanoindentation mechanical properties on spark plasma sintered 48Ti-48Al-2Cr-2Nb alloy

Mahlatse R. Mphahlele [a,b], Eugene Olevsky [c], Thato Tshephe [b], Peter A. Olubambi [b]

[a] Department of Mechanical Engineering, Durban University of Technology, Durban 4001, South Africa
[b] Centre of Nanomechanics and Tribocorrosion, School of Mining, Metallurgy & Chemical Engineering, University of Johannesburg, Doornfontein 2094, South Africa
[c] Powder Technology Laboratory, College of Engineering, San Diego State University, San Diego, CA, United States

ARTICLE INFO

Article history:
Received 16 April 2020
Received in revised form 17 July 2020
Accepted 28 July 2020
Available online 22 October 2020

Keywords:
Spark plasma sintering
Gamma TiAl
Nanoindentation
H/Er

ABSTRACT

This study aims to investigate the microstructure, plastic (H) properties, elastic (E) properties, reduced elastic (Er) properties the strain-to-break parameter (H/Er), and the resistance to plastic deformation parameter (H3/Er2) of the Ti-48Al-2Cr-2Nb alloy by use of scanning electron microscopy, nanoindentation and micro-indentation techniques. The results show that the sintering parameters had significant effect on the resulting microstructure. Desirable mechanical properties were obtained with the sample sintered at temperature of 1200 °C, pressure of 50 MPa, holding time of 7.5 min and a heating rate of 50 °C/min which had a near lamellar structure, resulting from the grain boundary pinning effect of the fine equiaxed gamma grains and the impartation of ductility due to the coarsened lamellar colonies. The nano-hardness and elastic modulus were observed to be about 4GPa and 31GPa for the near lamellar microstructure, respectively, with the microhardness of about 4.4GPa. While the duplex and the near gamma microstructures possessed the least nano-hardness (3.65–3.78GPa) and elastic modulus (3.6–29.5GPa) with the exception of sample sintered at temperature of 1150 °C, pressure of 50 MPa, holding time of 7.5 min and a heating rate of 100 °C/min., with nano-hardness and elastic modulus of 4.05GPa and 31.25GPa, respectively, however it had the lowest micro-hardness of 2.7GPa. Furthermore, the ratios H/Er and H3/Er2 values were observed to be greater for the same sample suggesting good wear resistance of the alloy.

Selection and peer-review under responsibility of the scientific committee of the International Symposium on Nanostructured, Nanoengineered and Advanced Materials.

1. Introduction

Gamma-titanium alloys are inherently characterised by their low densities and high stiffness which makes them ideal for various applications in aerospace and automobile industries. However, the alloys possess a number of limitations such as low ductility at room temperature, low surface hardness and poor tribological properties, which limits their wider applications in the mentioned areas especially where there is contact such as the valves in an auto- engine [1]. Various methods have been used to enhance their engineering properties, such as heat treatment, microstructural morphology control and alloying elements.

Several studies showed that alloying with transition metals, such as Cr, V, Mn, Fe, W, Mo, Nb, is an effective approach to solve the problem of low room temperature ductility [1]. Advanced TiAl alloys such as TNB alloy (Ti– 45Al–8Nb–0.2C%) and Ti4522XD(Ti–45Al–2Nb–2Mn–XD) are amongst several other TiAl alloy-systems that have been investigate [2]. The minor fractions of chromium (Cr) and niobium (Nb) were found to improve ductility and stiffness of the alloys and the fatigue strength of the cast and hot isostatic pressed TNB had exceptional

tolerance to defects than Ti–4522XD while the cast Ti–4522XD was shown to be unsuitable for applications because of excessive scatter in properties, due to variable microstructural features which could be as a result of the lengthy nature of casting processes. Consequentially, alternative methods have been investigated.

Amongst many methods available today to produce TiAl alloys, Spark plasma sintering (SPS) promise to facilitate the production of a gamma-TiAl having desirable microstructure and engineering properties. These advantageous aspects are conferred by the bene-

https://doi.org/10.1016/j.matpr.2020.07.738
2214-7853/
Selection and peer-review under responsibility of the scientific committee of the International Symposium on Nanostructured, Nanoengineered and Advanced Materials.

fits of SPS which includes short production periods and easily manipulated process parameters [3].

Mechanical property for gamma-TiAl produced with various techniques have previously been established to describe their deformation [4,5] and wear behaviour [1]. This has demonstrated that it is necessary to assess the gamma-TiAl alloys produced with the novel spark plasma sintering technique. Nanoindentation testing technique has proved to be a suitable method to investigate engineering property integrity of the alloys. The nanoindentation test provides the basic mechanical properties such as the hardness (H), the elastic modulus (E) as well as the E /H ratio which gives an indication of the material's wear behaviour. The aim of the study was to establish and present the nanoindentation behaviour of the spark plasma sintered gamma Ti-48Al-2Cr-2Nb alloy and derive the wear resistance behaviour from the nanoindentation data.

2. Experimental

The as-received titanium aluminide alloys used in this study had a nominal chemical compositions of (at.%) Ti- 48Al-2Cr-2Nb. The argon atomized powder used to produce the alloy samples was purchased from TLS Technik, and it had particle size of < 36 μm. Samples of about 20 mm in area and 5 mm in thickness were produced by spark plasma sintering of the powder under varied conditions; of temperature between 1150 and 1200, constant pressure of 50 MPa, heating rate of 50 and 100 and holding time of 5 min and 7.5 min, sample identities are summarised in Table 1.

The samples were then wet ground with silicon carbide (SiC) paper down to 1200 grit and polished with 0.2 μm silica suspension to obtain a mirror surface finish. A 401 etchant (a combination of bromine-methanol, sulphuric acid, phosphoric acid, hydrogen peroxide and water) was used to reveal the microstructure evolved

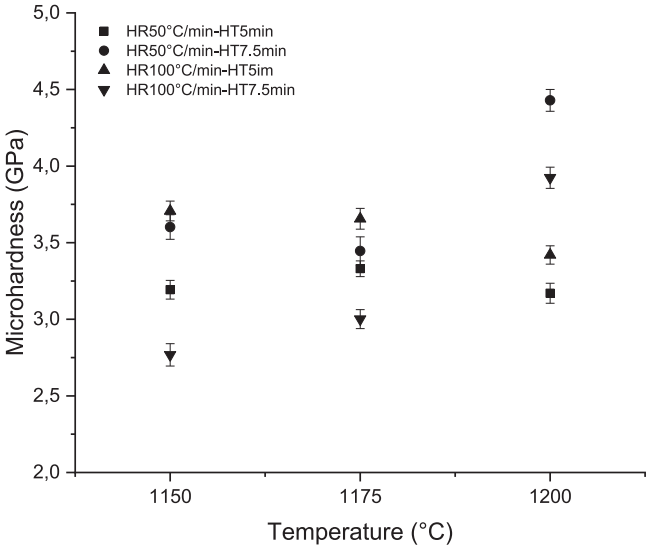

Fig. 2. Microhardness of the as-sintered TiAl, sintered at 1150 °C, 1175 °C and 1200 °C, with varied heating rate and holding time.

Table 1
Sample identity and their sintering parameters.

Sample ID	A	B	C	D	E	F	G	H	I	J	K	L
Temperature (T), °C	1150	1175	1200	1150	1175	1200	1150	1175	1200	1150	1175	1200
Heating rate (HR), °C/min	50	50	50	50	50	50	100	100	100	100	100	100
Holding time (HT),	5	5	5	7.5	7.5	7.5	5	5	5	7.5	7.5	7.5

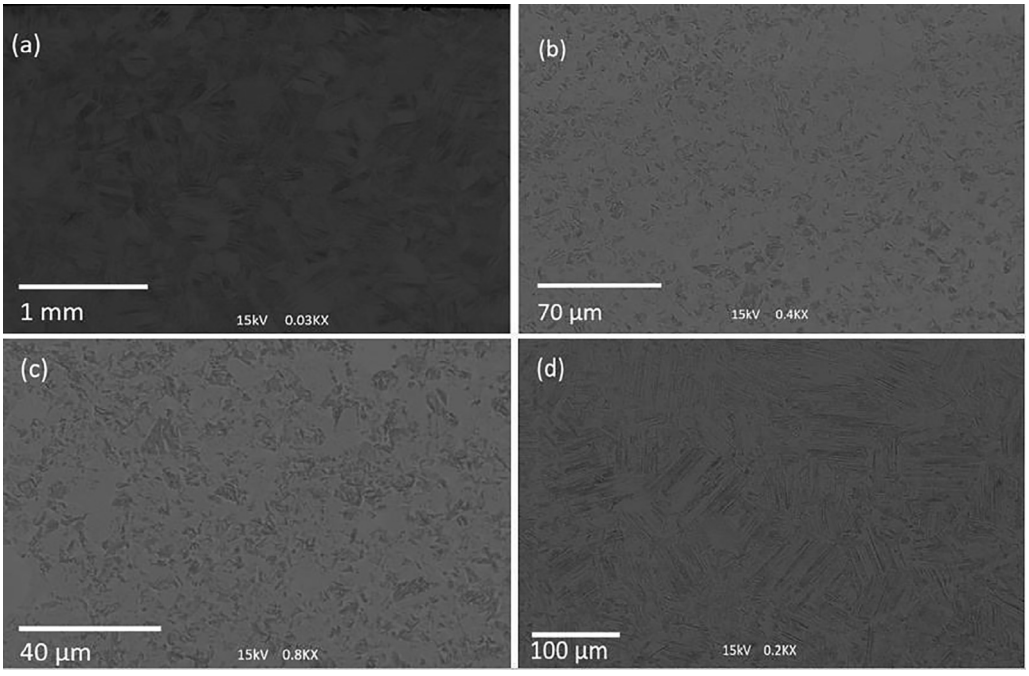

Fig. 1. SEM back scattered electron image of TiAl alloy sintered at, (a) T1150°C-50 MPa-HT5min-HR50°C/min (sample A), (b)T1175°C- 50 MPa-HT5min-HR100°C/min (sample H), (c) T1175°C-50 MPa-HT7.5 min-HR100°C/min (sample K), (d)T1200°C-50 MPa-HT7.5 min- HR50°C/min (sample F).

under the different processing conditions for examination by scanning electron microscopy - backscattering electron (Zeiss EVO 15). The evolved phases were characterised using X-ray diffractometry (XRD), a system of the PANalytical X'Pert HighScore.

Nanoindentation tests were performed on the metallographically prepared samples using Anton Paar ultra- Nanoindenter (UNHT) with a diamond Berkovich diamond indenter. A force control mode was selected in accordance with [6] to reach the peak force of 100mN. The matrix profile was used to make the 5×5 mapping indents. The load was maintained at the peak value for 10 s, and then unloaded to zero. The load–displacement curves were recorded continuously by the system and based on the Oliver and Phaar method [7], hardness and reduced elastic modulus were derived from the curves. Additionally, the wear resistance of the alloys were estimated using H/E_r and H^3/E_r^2 ratios [8,9].

3. Results and discussions

3.1. Microstructure analysis

Microstructural investigation using SEM back-scattering showed the effect of temperature, heating rate and holding time on the as-sintered microstructure of the Ti-48Al-2Cr-2Nb alloys. As shown in Fig. 1(a) the alloy sintered at 1150 °C presented a duplex structure having a co-existence of the equiaxed gamma grains and lamellar colonies. This dual phase structure has been found to be greatly influenced by lamellar spacing, thickness of the lamellas, volume fraction of microstructures and grain sizes will influence the mechanical properties [[10,11]. An increase in temperature to 1175 °C resulted in evolution of the near gamma structure (Fig. 1b & c) having equiaxed gamma grains ranging between 20 μm to 40 μm. The microstructure is formed when the material is subjected to at low temperatures heat-treated in the $\alpha + \gamma$ phase field [10]. Shown in Fig. 1(d) is a nearly lamellar structure which evolved on increase in temperature to 1200 °C. A coarsened lamellar colonies with minor amounts of fine equiaxed gamma grains can be observed on the microstructure with the grain size in the range of 50 μm to 100 μm.

3.2. Micro-Hardness and Nano-Hardness properties

Fig. 2 shows the micro-hardness of the sintered alloys in relation to their sintering parameters. The hardness of the alloys follows no definite trend, and it could be observed that the lowest hardness is found in the sample sintered at 1150° with a heating rate of 100 °C/min and holding time of 7.5 min (sample J). This hardness behaviour in the sample is due possibly low densification achieved by the low sintering temperature and pressure and grain coarsening from the long holding time (Table 1) while the highest hardness is demonstrated by the sample produced at temperatures of 1200 °C, heating rate of 50 °C and a holding time of 7.5 min (sample F) due to its favourable microstructural morphology (Fig. 1d). The sample sintered at temperature of 1150 °C with heating rate of 50 °C/min and holding time of 5 min (sample A), only has hardness of about 3.2GPa due combined contribution of its

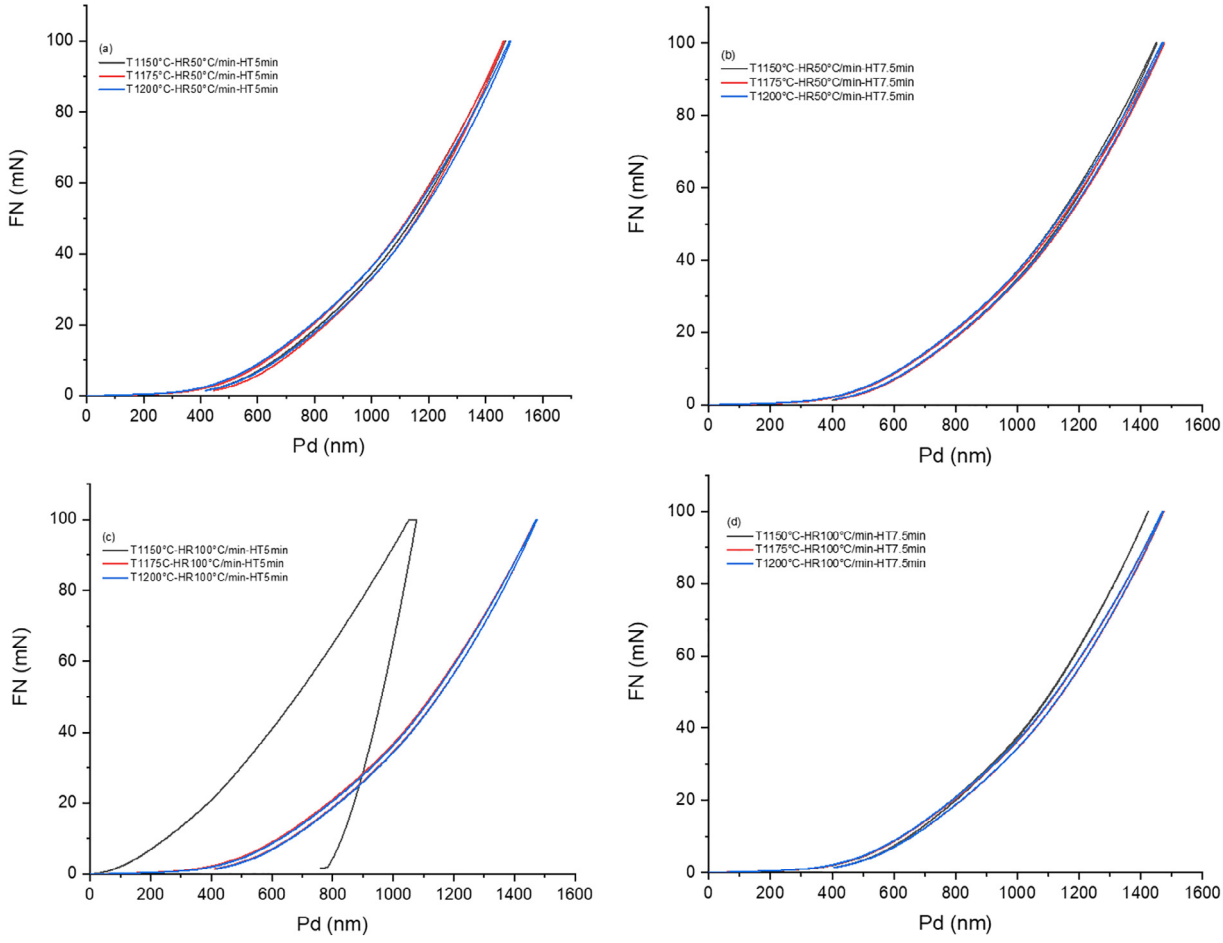

Fig. 3. Load-displacement curves of the TiAl alloys sintered at 1150 °C, 1175 °C and 1200 °C, (a) with heating rate of 50 °C/min and holding time of 5 min, (b) with heating rate of 50 °C/min and holding time of 7.5 min, (c) with heating rate of 100 °C/min and holding time of 5 min, (d) with heating rate of 100 °C/min and holding time of 7.5 min.

low relative density and the presence of the duplex microstructure (Fig. 1a) which has fairly coarse grain in the range of 0.1 mm to 0.3 mm. The hardness is observed to have a good link to the microstructure, which is expected as materials hardness properties are dependent on the morphology of the microstructure which are a function of its production conditions.

Fig. 3 shows the variations of indentation depth with indentation load on the spark plasma sintered TiAl alloys. As can be observed, the total indentation depth of all the samples except the sample sintered at temperature of 1175 °C with a heating rate of 50 °C/min and holding time of 5 min (sample B), lies in the range of 400 nm to 450 nm with sample A only somewhat distinctively displaying the uppermost indentation depth within the range and this could be due to its limited densification (Fig. 2) and the association with the ductile nature of the coarsened microstructure (Fig. 1a). An increase in the indentation depth with load for the sample B despite having relative microhardness of 3.3GPa which is higher than that of other several samples (A, C, J and K; refer to Table 1 for sintering parameters), as shown in Fig. 2, could be as a result of the effect of indentation pile up. This behaviour is characterised by an increase in hardness, in this case observed by the low indentation depth in the loading section followed by a decline in hardness with increasing indentation depth.

The nanoindentation hardness and elastic modulus as determined by the method of Oliver & Phaar (Oliver and Pharr 1992) are shown in Fig. 4. All samples display a good link between the indentation hardness and the elastic modulus, as the increase in hardness showed an increase in modulus of elasticity and vice versa owing to the inherent functional dependence of hardness on elastic modulus (Cheng and Cheng 1998). However, it should be noted that the lower nanoindentation hardness and elastic modulus observed with the sample sintered at temperature of 1175 °C with a heating rate of 50 °C/min and holding time of 5 min (sample B), can be attributed to the pile-up of indentation size effect which is usually observed in samples having lower elastic modulus. Most importantly, the sample had residual depth/-maximum depth (hf/hmax) value of about 0.83 as presented in Fig. 5. This is consistent with common experiences (Bolshakov and Pharr 1998, Qian, Li et al. 2005) which have established that pile-up effects usually occur in materials with hf/hmax values greater than 0.7. Whilst sample sintered at 1150° with a heating rate of 100 °C/min and holding time of 7.5 min (sample J) shows the highest indentation hardness and elastic modulus, despite having the lowest bulk hardness (HV) as shown in Fig. 2. It is often the case that discrepancies between the nanoindentation hardness & and Vickers hardness occur due to the different definitions of contact area in Vickers hardness and nanoindentation hardness, mainly because the calculation of contact area in HV neglects the difference in pile-up/sink-in effects which are rather essential in deriving the nanoindentation hardness (Kang, Kim et al. 2010). Samples produced under temperature of 1150 °C were observed

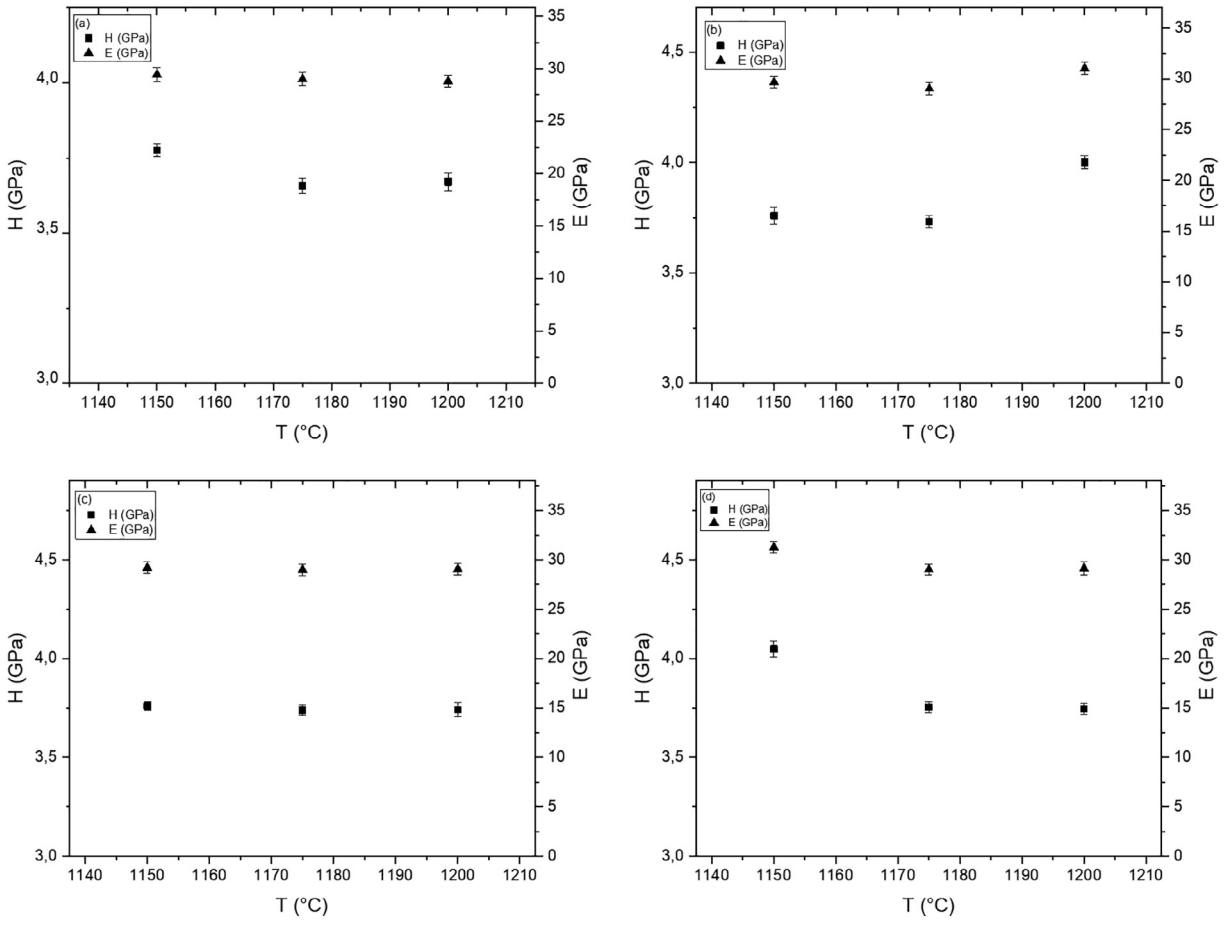

Fig. 4. Nanoindentation hardness and elastic modulus of the as-sintered TiAl alloys, sintered at 1150 °C, 1175 °C and 1200 °C, (a) with heating rate of 50 °C/min and holding time of 5 min, (b) with heating rate of 50 °C/min and holding time of 7.5 min, (c) with heating rate of 100 °C/min and holding time of 5 min, (d) with heating rate of 100 °C/min and holding time of 7.5 min.

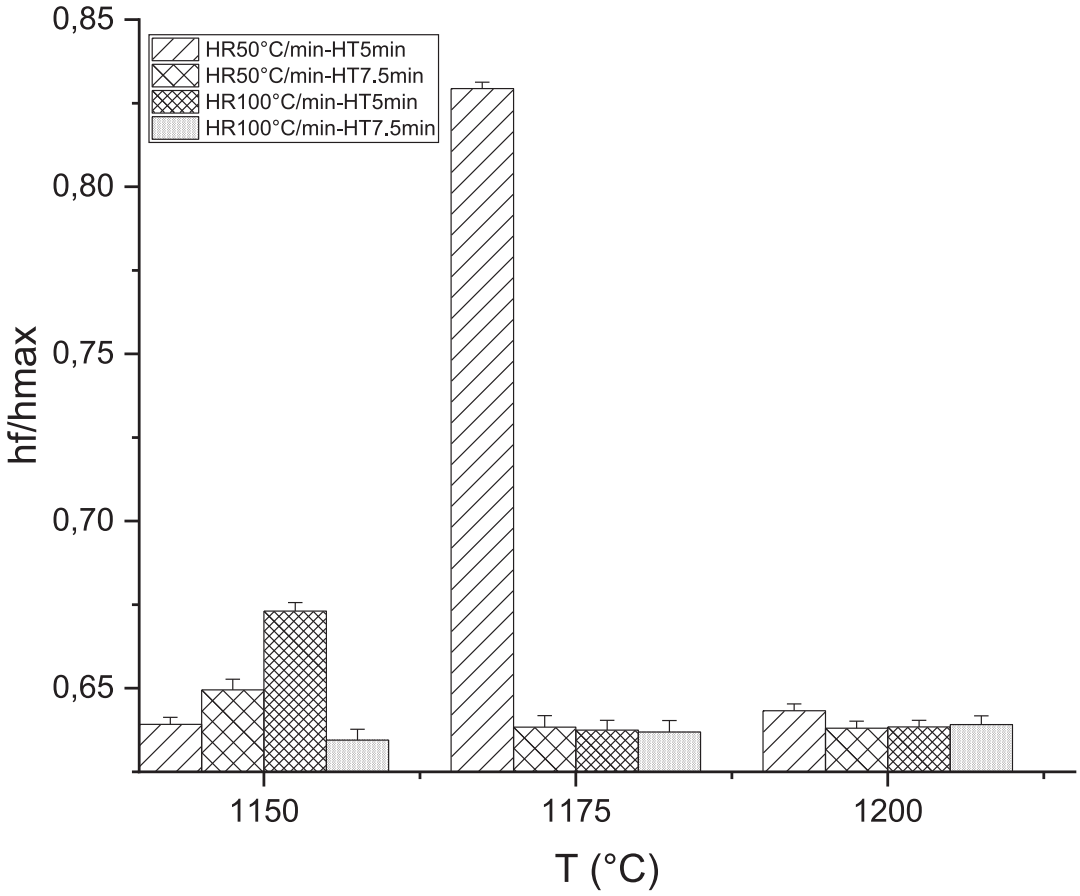

Fig. 5. Depth dependence ratio for as-sintered TiAl alloys for load of 100mN.

to display a duplex structure (i.e. Fig. 1a) which is characterised by increase in ductility although this comes at the compromise of creep properties (Clemens and Mayer 2013).

4. Projected wear behaviour of TiAl alloys

A great deal of the physics of hardness considers hardness to be the primary property which describes the resistance of a material to wear [12]. Accordingly, the ratio of hardness to elastic modulus, H/Er, is of momentous interest in both tribology and fracture mechanics. Several authors [13,14], have demonstrated that the ratios H/E_r (elastic strain to failure) and H^3/E_r^2 (yield pressure) are suitable parameter to define the wear resistance of a material. The results of H/E_r and H^3/E_r^2 calculated from the H and E_r values for the TiAl alloys sintered at various conditions are presented in Fig. 6. The ratios H/E_r and H^3/E_r^2 ratios were noted to be higher for the alloys with high indentation hardness (i.e sample F and sample J). The ratios are more pronounced with sample F, this is expected due to the high hardness. A previously discussed, this is due to the presence of the fine equiaxed gamma grains within the coarsened lamellar colonies which are effective in restraining dislocation movement through the material.

5. Conclusions

This work investigated nanoindentation and mechanical properties of Ti-48Al-2Cr-Nb produced by spark plasma sintering. The SEM back scattered electrons revealed the evolution of the microstructure with varied sintering conditions. The nanoindentation results revealed that plastic (H) property, elastic (E) property, the strain-to-break parameter (H/Er), and the resistance to plastic deformation parameter (H^3/Er^2) of the TiA alloy was significantly influenced by the morphology of the evolved microstructure. This is evident by the results from which it is concluded that nearly lamellar structure consisting of coarsened lamellar colonies with minor amounts of fine equiaxed gamma grains improved the nanohardness, microhardness and resistance to elastic strain to failure (measure of wear) in the alloys. Estimation of the stress strain properties using nanoindentaion data and nano-micro hardness correlations will be reported elsewhere.

CRediT authorship contribution statement

Mahlatse R. Mphahlele: Conceptualization, Methodology, Validation, Investigation. **Eugene Olevsky:** Supervision. **Thato Tshephe:** Resources. **Peter A. Olubambi:** Conceptualization, Supervision.

Declaration of Competing Interest

The authors declare that they have no known competing financial interests or personal relationships that could have appeared to influence the work reported in this paper.

Acknowledgements

The authors would like to extend appreciation to National Research Foundation (NRF) for financial support.

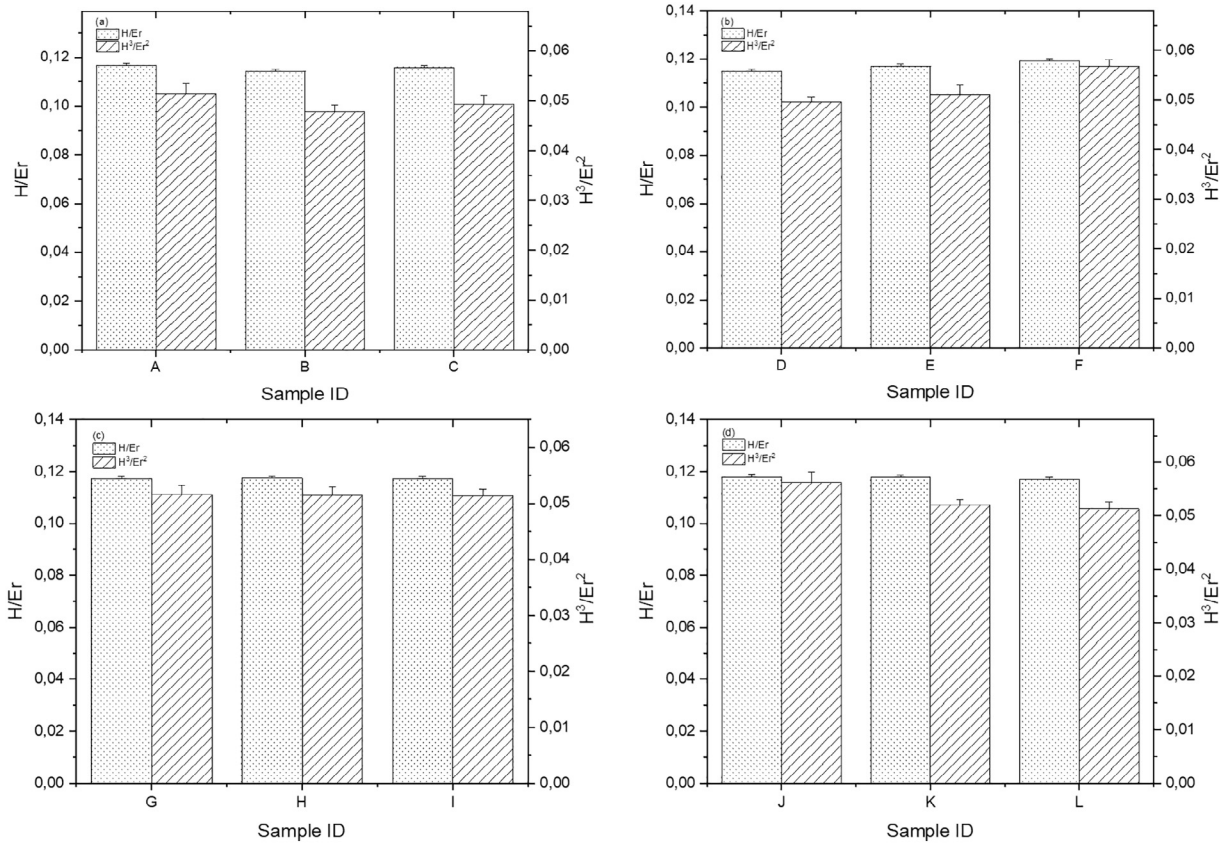

Fig. 6. H/Er and H^3/Er^2 ratios of the as-sintered TiAl alloy.

References

[1] J. Xia et al., Nanoindentation and nanoscratch properties of a thermal oxidation treated γ-TiAl based alloy, Surf. Coat. Technol. 200 (16–17) (2006) 4755–4762.

[2] W.E. Voice et al., Gamma titanium aluminide, TNB, Intermetallics 13 (9) (2005) 959–964.

[3] M. Eriksson, M. Radwan, Z. Shen, Spark plasma sintering of WC, cemented carbide and functional graded materials, Int. J. Refract Metal Hard Mater. 36 (2013) 31–37.

[4] W. Li et al., Indentation response of γ-TiAl (111) and influence of True-twin interface, Procedia Manuf. 37 (2019) 190–194.

[5] S. Fager Franzén, and J, Karlsson, Titanium Aluminide Manufactured by Electron Beam Melting, 2010.

[6] X. Li, B. Bhushan, A review of nanoindentation continuous stiffness measurement technique and its applications, Mater. Charact. 48 (1) (2002) 11–36.

[7] W.C. Oliver, G.M. Pharr, An improved technique for determining hardness and elastic modulus using load and displacement sensing indentation experiments, J. Mater. Res. 7 (6) (1992) 1564–1583.

[8] J. Chen, S. Bull, Relation between the ratio of elastic work to the total work of indentation and the ratio of hardness to Young's modulus for a perfect conical tip, J. Mater. Res. 24 (3) (2009) 590–598.

[9] J. Chen, S. Bull, A critical examination of the relationship between plastic deformation zone size and Young's modulus to hardness ratio in indentation testing, J. Mater. Res. 21 (10) (2006) 2617–2627.

[10] K. Kothari, R. Radhakrishnan, N.M. Wereley, Advances in gamma titanium aluminides and their manufacturing techniques, Prog. Aerosp. Sci. 55 (2012) 1–16.

[11] Y.-W. Kim, D.M. Dimiduk, Progress in the understanding of gamma titanium aluminides, Jom 43 (8) (1991) 40–47.

[12] S. Abdi et al., Effect of Nb addition on microstructure evolution and nanomechanical properties of a glass-forming Ti–Zr–Si alloy, Intermetallics 46 (2014) 156–163.

[13] S. Ehtemam-Haghighi, G. Cao, L.-C. Zhang, Nanoindentation study of mechanical properties of Ti based alloys with Fe and Ta additions, J. Alloy. Compd. 692 (2017) 892–897.

[14] M. Masanta, S. Shariff, A.R. Choudhury, Evaluation of modulus of elasticity, nano-hardness and fracture toughness of TiB2–TiC–Al2O3 composite coating developed by SHS and laser cladding, Mater. Sci. Eng., A 528 (16–17) (2011) 5327–5335.